



ELSEVIER

Contents lists available at ScienceDirect

Redox Biology

journal homepage: www.elsevier.com/locate/redoxRobust rat pulmonary radioprotection by a lipophilic Mn N-alkylpyridylporphyrin, MnTnHex-2-PyP⁵⁺ ☆Benjamin Gauter-Fleckenstein ^{a,b}, Julio S. Reboucas ^{a,1}, Katharina Fleckenstein ^{a,b}, Artak Tovmasyan ^a, Kouros Owzar ^{c,d}, Chen Jiang ^d, Ines Batinic-Haberle ^{a,*}, Zeljko Vujaskovic ^{a,e,**}^a Department of Radiation Oncology, Duke University School of Medicine, Durham, NC 27710, USA^b Department of Radiation Oncology, Universitätsmedizin Mannheim, Medical Faculty Mannheim, Heidelberg University, Mannheim, Germany^c Department of Biostatistics and Bioinformatics, Duke University Medical Center, Durham, USA^d Biostatistics and Computational Biology Core, RadCCORE, Duke University Medical Center, Durham, USA^e Division of Translational Radiation Sciences, Department of Radiation Oncology, University of Maryland, 655W Baltimore Street, Bressler Research Building, 8-025, Baltimore, MD 21201, USA

ARTICLE INFO

Article history:

Received 3 December 2013

Received in revised form

19 December 2013

Accepted 20 December 2013

Keywords:

Radioprotection

Fischer rats

Manganese porphyrins

MnTnHex-2-PyP⁵⁺MnTE-2-PyP⁵⁺

Redox-modulators

Lung injury

Immunohistochemistry

Histopathology

Breathing frequencies

ABSTRACT

With the goal to enhance the distribution of cationic Mn porphyrins within mitochondria, the lipophilic Mn(III)meso-tetrakis(*N*-hexylpyridinium-2-yl)porphyrin, MnTnHex-2-PyP⁵⁺ has been synthesized and tested in several different model of diseases, where it shows remarkable efficacy at as low as 50 µg/kg single or multiple doses. Yet, in a rat lung radioprotection study, at higher 0.6–1 mg/kg doses, due to its high accumulation and micellar character, it became toxic. To avoid the toxicity, herein the pulmonary radioprotection of MnTnHex-2-PyP⁵⁺ was assessed at 50 µg/kg. Fischer rats were irradiated to their right hemithorax (28 Gy) and treated with 0.05 mg/kg/day of MnTnHex-2-PyP⁵⁺ for 2 weeks by subcutaneously-implanted osmotic pumps, starting at 2 h post-radiation. The body weights and breathing frequencies were followed for 10 weeks post-radiation, when the histopathology and immunohistochemistry were assessed. Impact of MnTnHex-2-PyP⁵⁺ on macrophage recruitment (ED-1), DNA oxidative damage (8-OHdG), TGF-β1, VEGF(A) and HIF-1α were measured. MnTnHex-2-PyP⁵⁺ significantly decreased radiation-induced lung histopathological (H&E staining) and functional damage (breathing frequencies), suppressed oxidative stress directly (8-OHdG), or indirectly, affecting TGF-β1, VEGF (A) and HIF-1α pathways. The magnitude of the therapeutic effects is similar to the effects demonstrated under same experimental conditions with 120-fold higher dose of ~5000-fold less lipophilic Mn(III)meso-tetrakis(*N*-ethylpyridinium-2-yl)porphyrin, MnTE-2-PyP⁵⁺.

© 2014 The Authors. Published by Elsevier B.V. This is an open access article under the CC BY-NC-ND license (<http://creativecommons.org/licenses/by-nc-nd/3.0/>).

Abbreviations: GMP, good manufacturing practice; CNS, central nervous system; SAH, subarachnoid hemorrhage; I/R, ischemia reperfusion; AT, ataxia telangiectasia; ALS, amyotrophic lateral sclerosis; NOX4, NADPH oxidase, isoform 4; E_{1/2}, Half-wave metal-centered reduction potential; SOD, superoxide dismutase; NHE, normal hydrogen electrode; SOD, superoxide dismutase; ONOO⁻, peroxynitrite; O₂⁻, superoxide; NO, nitric oxide; CO₃⁻, carbonate radical; HO₂⁻, monodeprotonated hydrogen peroxide; ClO⁻, hypochlorite; GS⁻, monodeprotonated glutathione; MnP, Mn porphyrin; MnTnHex-2-PyP⁵⁺, Mn(III) meso-tetrakis(*N*-hexyl)pyridinium-2-yl)porphyrin (AEOL10113); MnTE-2-PyP⁵⁺, Mn(III) meso-tetrakis(*N*-ethylpyridinium-2-yl)porphyrin (AEOL10113); MnTnBuOE-2-PyP⁵⁺, Mn(III) meso-tetrakis(*N*-*n*-butoxyethyl)pyridinium-2-yl)porphyrin; MnTDE-2-ImP⁵⁺, Mn(III) tetrakis[*N,N*-diethylimidazolium-2-yl)porphyrin, AEOL10150; HIF-1α, hypoxia inducible factor-1; NF-κB, nuclear factor κB; AP-1, activator protein-1; SP-1, specificity protein-1; TGF-β1, one of the 3 members of the TGF-β transforming growth factor-β family; TF, transcription factor; Nrf-2, nuclear factor-erythroid-derived 2-like 2; VEGF, vascular endothelial growth factor; PTEN, phosphoinositide 3-phosphatase; MCAO, middle cerebral artery occlusion; 8-OHdG, 8-hydroxy-2'-deoxyguanosine; PI3K, phosphatidylinositol 3-kinase; AKT, protein kinase B (PKB), a serine/threonine-specific protein kinase; mTOR, mammalian target of rapamycin (mTOR), a serine/threonine protein kinase; ETC, mitochondrial electron transport chain; BBB, blood brain barrier

^{*}This is an open-access article distributed under the terms of the Creative Commons Attribution-NonCommercial-No Derivative Works License, which permits non-commercial use, distribution, and reproduction in any medium, provided the original author and source are credited.

^{*} Correspondence to: Department of Radiation Oncology, Duke University School of Medicine, Research Drive, MSRB 1, 281b, Durham, NC 27710, USA.

^{**} Corresponding author at: University of Maryland, Division of Translational Radiation Sciences, Department of Radiation Oncology, 655W Baltimore Street, Bressler Research Building, 8-025, Baltimore, MD 21201, USA. Tel.: +1 410 706 5139; fax: +1 410 706 6666.

¹ Present address: Departamento de Quimica, CCEN, Universidade Federal da Paraiba, Joao Pessoa, Paraiba, Brazil.

<http://dx.doi.org/10.1016/j.redox.2013.12.017>

2213-2317 © 2014 The Authors. Published by Elsevier B.V. This is an open access article under the CC BY-NC-ND license (<http://creativecommons.org/licenses/by-nc-nd/3.0/>).

Introduction

The normal tissue surrounding tumor suffers substantial damage during anticancer therapy, which limits radiation dose and thus the magnitude of therapeutic effects. There is still an unmet need for the efficacious radioprotector of a normal tissue. Such a compound will also be invaluable in the cases of accidental nuclear exposures. Thus radioprotectors have been actively sought by a number of groups [1–6]. We have demonstrated the therapeutic efficacy of cationic Mn(III) *N*-substituted pyridylporphyrins (MnPs) in various animal models of diseases, radiation injury included, which all have oxidative stress in common [2,7,8]. MnPs are among the most potent metal-based SOD mimics thus far developed. While data suggests that O_2^- might not be always the only and/or major species involved in their mechanism of action, the ability of MnPs to catalyze the O_2^- dismutation, described by the rate constant for the catalysis of O_2^- dismutation by MnP, $k_{cat}(O_2^-)$, parallels their ability to exhibit therapeutic effects in all diseases thus far tested. The latter is related to their favorable properties which allow them to readily exchange electrons with cellular reductants, reactive species and redox-active signaling proteins. For details the reader is advised to see the most updated review on the mechanisms of action of SOD mimics and their radioprotective and anticancer effects (Forum issue on “SOD mimics” of *Antioxid Redox Signal* [2]). The facile exchange of electrons with bio-targets is controlled by the thermodynamic property of Mn porphyrin, i.e. the reduction potential of Mn^{III}/Mn^{II} redox couple, $E_{1/2}$, and the kinetic property ($k_{cat}(O_2^-)$). Both properties are controlled by the placement of cationic charges in the close vicinity of Mn site on the *ortho* pyridyl nitrogens (Fig. 1) [2,9]. Such placement of charges attracts anionic reactive species (O_2^- , $ONOO^-$, HO_2^- , ClO^- , GS^- , RS^-) to the metal site where redox chemistry/biology occurs.

The MnTE-2-PyP⁵⁺ (AEOL10113) was the very first developed and thus far the most studied cationic Mn(III) *N*-substituted pyridylporphyrin [1,10–12]. Based on the same thermodynamic and kinetic principles, the similarly hydrophilic *N,N*-dialkylimidazolium analog, MnTDE-2-ImP⁵⁺ (AEOL10150) has been developed and successfully tested in different in vitro and in vivo models of oxidative stress injuries [13–17]. With a goal to increase mitochondrial and brain accumulation while maintaining the favorable redox property of the metal site and the positive charges, the ~5000-fold more lipophilic MnTnHex-2-PyP⁵⁺ was synthesized [18] and successfully tested in different diseases (summarized in Fig. 1). The pharmacokinetic data clearly show that more lipophilic compounds distribute to higher levels in key cellular fragments – mitochondria: MnTE-2-PyP⁵⁺ (Fig. 1) distributes 1.5-fold more in mouse heart mitochondria relative to cytosol, while for MnTnHex-2-PyP⁵⁺ the mitochondrial to cytosolic ratio is 3.6 [2]. The higher mitochondrial accumulation likely contributes to up to 120-fold larger therapeutic effects of MnTnHex-2-PyP⁵⁺ than of MnTE-2-PyP⁵⁺. The same property that facilitates the transport of MnP across the mitochondrial membranes – cationic charge and lipophilicity – allows it to cross the blood brain barrier and exert protection in injuries of central nervous system. The toxicity dose, TD_{50} , at which 50% of mice developed signs of disease, is 91.5 mg/kg (given sc) for MnTE-2-PyP⁵⁺ and 12.5 mg/kg for MnTnHex-2-PyP⁵⁺ [19]. Toxicity was demonstrated as hypotonia, and shaking. The ratio of maximal tolerable dose to the lowest efficacious dose is 15 (91.5/6) for MnTE-2-PyP⁵⁺ vs 250 (12.5/0.05) for MnTnHex-2-PyP⁵⁺. The ratio 250/15 implies that the therapeutic window of MnTnHex-2-PyP⁵⁺ is ~17-fold larger than for MnTE-2-PyP⁵⁺ [1,2,12,19–21].

We recently reported the rat pulmonary radioprotection by those two Mn porphyrins [10,11]. While the most efficacious dose of MnTE-2-PyP⁵⁺ tested was 6 mg/kg/day, the MnTnHex-2-PyP⁵⁺ exhibited significant toxicity at doses of 0.6 and 1 mg/kg/day. The

daily subcutaneous injections of 0.6 and 1 mg/kg/day of MnTnHex-2-PyP⁵⁺ over a period of 14 days (starting at 2 h post-radiation) resulted in skin lesions, leading to local necrosis and alopecia. Even with the most efficacious daily dose of 0.3 mg/kg given over a 14 day-period, the significant loss of body weight was demonstrated. The therapeutic effect of MnP was diminished to a certain degree by such toxicity [10]. The toxicity was originally ascribed to the surfactant nature of MnP which allowed it to damage lipid bilayers of cellular membranes [1,7]. Meanwhile, the lack of dark toxicity of redox-inactive but similarly lipophilic analog, ZnTnHex-2-PyP⁵⁺ was demonstrated [22]. Therefore, the toxicity of MnTnHex-2-PyP⁵⁺ is likely linked to its higher lipophilicity and consequently higher accumulation inside the cell, where it could dose-dependently induce apoptotic processes. The ethyl and n-hexyl analogs differ significantly with respect to $E_{1/2}$ of $Mn^{III}P/Mn^{II}P$ redox couple also, the impact of which on the efficacy and toxicity waits further exploration (see Discussion).

Few animal studies, such as rat kidney ischemia/reperfusion and rabbit cerebral palsy, indicated that MnTnHex-2-PyP⁵⁺ has remarkable efficacy at as low as 0.05 mg/kg (single or multiple dosing) [23,24]. We therefore aimed herein to investigate whether 0.05 mg/kg/day of MnTnHex-2-PyP⁵⁺ might be more beneficial than 0.3 mg/kg/day in a rat irradiation-induced lung injury. The effects of 0.05 mg/kg/day of MnTnHex-2-PyP⁵⁺ were compared to those produced by 6 mg/kg of hydrophilic MnTE-2-PyP⁵⁺ [10].

The remarkable data provided in this study led to the non-human primate lung radioprotection study where 0.05 mg/kg of MnTnHex-2-PyP⁵⁺ was given twice daily for 4 months, starting at 24 h before radiation. The data demonstrated a significant pulmonary radioprotection [25]. A subsequent non-human primate study is in progress with maximal tolerable dose of 0.25 mg/kg/day (Cline et al., unpublished).

Methods

Animals

Twenty-four female Fischer-344 rats were used in this study with prior approval from the Duke University Institutional Animal Care and Use Committee. Three animals were housed per cage and maintained under identical conditions with food and water provided ad libitum. All rats were sacrificed ten weeks post-radiation by pentobarbital overdose.

SOD mimetic

MnTnHex-2-PyP⁵⁺ was synthesized and characterized as previously described [26]. The PBS solution of the manganese porphyrin was used in this study.

Irradiation and treatment with SOD mimetic

At the time of irradiation all rats weighed between 175 and 185 g to minimize possible variations in lung size. The 24 animals were divided equally into the following groups to receive: 1) right hemithoracic irradiation (IR), 2) no IR and PBS, 3) IR and MnTnHex-2-PyP⁵⁺ (0.05 mg/kg/day). Hemithoracic irradiation of the right lung with a single dose of 28 Gy using 150 kV X-rays with a dose rate of 0.71 Gy/min (Therapax 320, Pantak Inc., East Haven, CT) was performed as previously described [10,11,27]. Mn porphyrin as well as PBS were delivered for 14 days by subcutaneous implanted osmotic pumps (Alzet[®] Model 2ML2, Durect Corporation, Cupertino, CA) at a dose rate of 5.0 μ l/h (0.05 mg/kg/day) starting at 2 h after radiation. Relative to our previous experiences where MnTnHex-2-PyP⁵⁺ was injected subcutaneously [10], the controlled injection rate (5 μ l/min) via sc-implanted osmotic

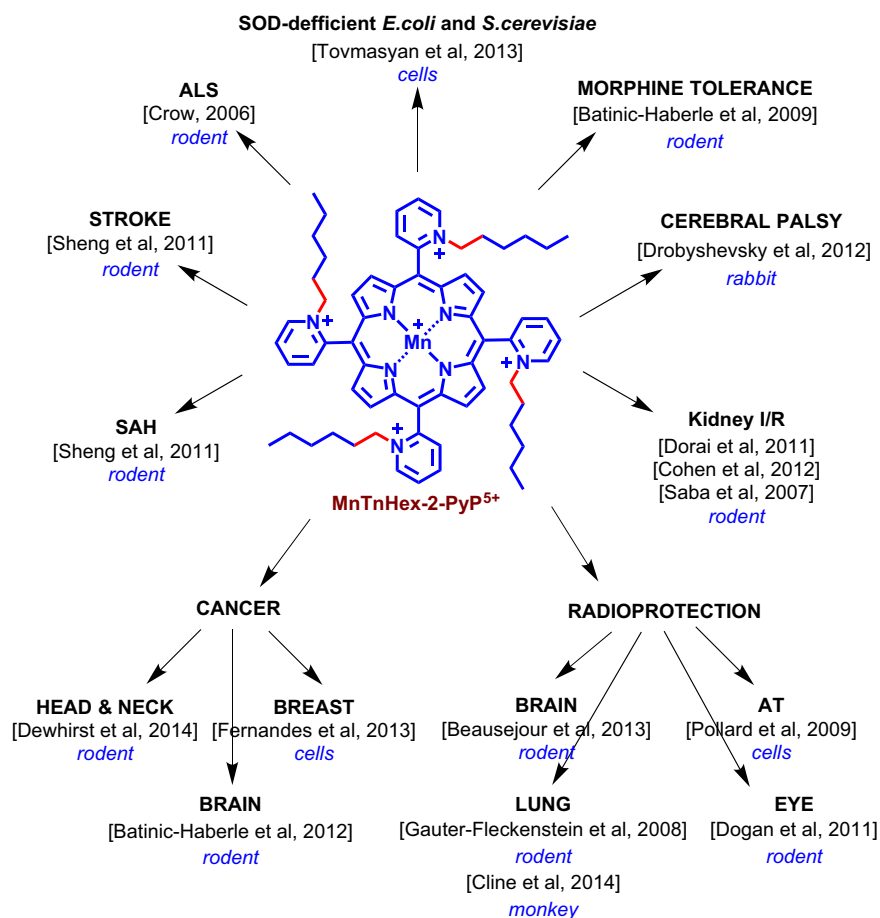


Fig. 1. Therapeutic effects of MnTnHex-2-PyP⁵⁺. The ethyl (E) compound, MnTE-2-PyP⁵⁺ has –CH₂–CH₃ chains attached to pyridyl nitrogens which are indicated with red bonds. SAH–Subarachnoid Hemorrhage; I/R – Ischemia/Reperfusion; AT – Ataxia Telangiectasia; ALS – Amyotrophic Lateral Sclerosis.

pumps was well tolerated. It did not cause any negative effects such as local alteration of pump implantation sites or weight loss.

Follow-up and functional assessment of lung injury

All animals were followed-up during ten weeks after IR. Body-weight was measured bi-weekly. Breathing frequency using whole-body plethysmography (Model RM-80, Columbus Instruments, Columbus, OH, USA) was measured as an indicator of pulmonary injury. Measurements were taken in a representative group ($n=10$) before IR and in 5 animals per group biweekly, starting 4 weeks after IR until week 10. The mean values of five measurements were recorded.

Histology

At the time of sacrifice, the right upper lobes of all animals were obtained for immunohistochemistry and histopathology studies. Animals were euthanized with pentobarbital overdose. Both lungs were infused by tracheal instillation of a solution containing 2% glutaraldehyde and 0.085 M sodium cacodylate buffer for 25 min for fixation prior to removal of the lung. After removal, the lobes of the irradiated right lung were separated and embedded in paraffin.

Histopathology and immunohistochemistry

Hematoxylin and eosin staining: Five-micrometer thick sections of the lung tissue, embedded in paraffin, were stained with hematoxylin and eosin (H&E). The extent of radiation-induced

damage for each field was graded on a scale from 0 (normal lung) to 8 (total obliteration of the field), as described by Ashcroft et al. [28]. Average scoring below grade 4 (moderate thickening of walls without obvious damage to lung architecture) resulted in the rat allocation in the “no damage” group, while average scoring above grade 4 (increased fibrosis with definite damage to lung architecture) led to the respective rat placement in the “damage” group.

Immunohistochemistry of lungs was done as previously described [10,11,14,27]. Lungs were assessed for the number and activity of macrophages with ED-1 staining, the expression of 8-OHdG (8-hydroxy-2'-deoxyguanosine) as a marker of oxidatively modified DNA, expression of TGF- β 1 (transforming growth factor- β 1), a profibrogenic cytokine, and HIF-1 α (hypoxia inducible factor 1 α), a pro-angiogenic transcription factor and its product VEGF(A) (vascular endothelial growth factor A), a pro-angiogenic cytokine.

Immunohistochemistry was performed as described by Hsu et al. [29]. The primary antibodies used, were directed against activated macrophage marker ED1 (MCA341, 1:100, Serotec, Oxford, UK), 8-OHdG (MOG-020P, 1:1000, JaiCA, Shizuoka, Japan), VEGF(A) (Sc-152, 1:100, Santa Cruz Biotechnology Inc., Santa Cruz, CA), active TGF- β 1 (Sc-146, 1:200, Santa Cruz Biotechnology Inc., Santa Cruz, CA), and HIF-1 α (NB 100-105, 1:100, Novus Biologicals, Littleton, CO). Image analysis was carried out as previously described [10,11]. Results were expressed as the number of positively stained macrophages or as percentage of 8-OHdG or HIF-1 α -positive nuclei per digital image (average of eight digital images per animal, average of five or six animals per group). For TGF- β and VEGF(A), the results represent the average percentage of positive staining (the ratio of positive staining over the total tissue area per digital image).

Statistical analysis

The discrepancies between binomial proportions were tested using Fisher's exact test [30]. The distributions of the biomarkers with respect to the drug (or dose) were compared in a pairwise fashion using the exact two-sample Wilcoxon test [31]. For breathing frequencies and body weight, an aggregate measure was computed as the empirical area under the curve. The distributions of these curves were compared in a pairwise fashion using the exact two-sample Wilcoxon test [31]. The R statistical environment [32] was used for all statistical analyses.

Results

Body weight and breathing frequencies

The control non-irradiated rats gain weight more than the irradiated group for most of a 10 week-period of observation. Even for a large period of time rats irradiated but treated with MnP gained weight in a similar fashion as non irradiated non MnP-treated rats (Fig. 2, Table 1). Average starting body weight across all groups was 181.1 ± 2.2 g at day of IR. The non-irradiated control group gained undisturbed weight throughout the entire process. In contrast, animals which were irradiated but received no treatment (IR only-group) gained significantly less weight ($p=0.012$ vs. PBS only). Animals which were irradiated and treated with MnTnHex-2-PyP⁵⁺ displayed higher body weight in comparison with the untreated irradiated animals ($p=0.004$ vs IR only-group). In contrast, animals which received MnTE-2-PyP⁵⁺ showed only a trend towards higher body weight in comparison with the IR only-group ($p=0.129$ vs. IR only-group). This is in agreement with what we saw in other studies where low levels of MnPs produce benefit to wild type *E. coli* and different cancer cell lines [33,34]. Nevertheless, animals from the IR+MnTE-2-PyP⁵⁺-group displayed a slightly decreased starting body weight in comparison with most other groups. When the trajectories depicting body weight over ten weeks were compared between MnTE-2-PyP⁵⁺ and MnTnHex-2-PyP⁵⁺ treatment groups, no difference could be observed ($p=0.487$ for IR+MnTE-2-PyP⁵⁺-group vs IR+MnTnHex-2-PyP⁵⁺-group) (Fig. 2; *p* values Table 1).

Significantly higher breathing rates were measured in the IR only-group ($p=0.008$ vs. control group). In stark contrast, animals which were treated with MnTnHex-2-PyP⁵⁺ (0.05 mg/kg) starting 2 h after IR did not display any changes in breathing frequencies relative to control group (Fig. 3; $p=0.008$ for IR+MnTnHex-2-PyP⁵⁺ vs IR only-group). Also, animals which received MnTE-2-PyP⁵⁺ (6 mg/kg) displayed significantly decreased breathing frequencies in comparison to the IR only-group ($p=0.008$ for IR+MnTE-2-PyP⁵⁺ vs IR only-group). Nevertheless, in direct comparison animals which received MnTnHex-2-PyP⁵⁺ after IR revealed significantly lower breathing frequencies in comparison to the IR+MnTE-2-PyP⁵⁺ group ($p=0.032$) signifying less functional damage in this group (Fig. 3; *p* values in Table 1).

Histopathology and immunohistochemistry

H&E staining showed no damage in the control group (average scoring grade=0.29 for PBS only). In comparison, 10 weeks after RT the average damage scoring for animals in the IR-only group was 5.3 (min 0, max 8), i.e., 85% of all animals in this group displayed significant histopathological damage (scoring >4, describing obvious damage to lung structure [28]). The damage was composed of severe distortion of lung structure, accumulation of alveolar macrophages, interstitial/alveolar edema, and beginning of the formation of fibrous masses. Animals in both

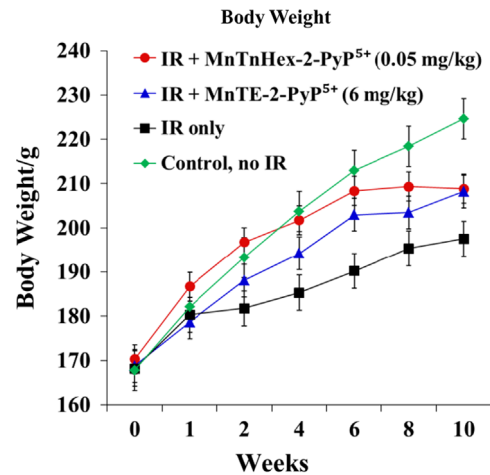


Fig. 2. The changes in body weight over 10 weeks (starting at 2 h post-IR) for rats which are irradiated and treated (for 14 days starting at 2 h post-IR) with 0.05 mg/kg/day of MnTnHex-2-PyP⁵⁺ in comparison with 6 mg/kg/day of MnTE-2-PyP⁵⁺. The IR only-group gained significantly less weight ($p=0.012$ vs. PBS only). The IR+MnTnHex-2-PyP⁵⁺ group displayed higher body weight in comparison with the untreated irradiated animals ($p=0.004$ vs IR only-group). In contrast, animals which received MnTE-2-PyP⁵⁺ starting 2 h after IR showed only a trend towards higher body weight in comparison with the IR only-group [11].

Table 1

The statistical analysis of the data obtained for the treatment of irradiated rats with 0.05 mg/kg/day for MnTnHex-2-PyP⁵⁺ in comparison to the data obtained for rats treated with 6 mg/kg/day of MnTE-2-PyP⁵⁺ [11]. The weights and breathing frequencies (respiration rate) were followed continuously (Figs. 2 and 3), while all other analyses were done at 10 weeks post-IR. The *p* values of parameters tested by histopathology (HP) and immunohistochemistry (IHC) studies, body weight, and breathing frequencies.

	Endpoint	Stat. Test	No IR, PBS	IR, MnTE-2-PyP ⁵⁺	IR, MnTnHex-2-PyP ⁵⁺	MnTE-2-PyP ⁵⁺ vs. MnTnHex-2-PyP ⁵⁺
HP	H & E	RST	0.002	0.026	0.009	1.000
	H & E	Fisher	0.002	0.061	0.061	1.000
IHC	ED-1	RST	0.002	0.179	0.015	0.818
	8-OHdG	RST	0.002	0.002	0.009	0.015
	TGF-β1	RST	0.002	0.002	0.002	0.065
	HIF-1 α	RST	0.002	0.002	0.132	0.240
	VEGF (A)	RST	0.002	0.002	0.009	0.818
Weight		RST	0.012	0.129	0.004	0.487
	Resp. Rate	RST	0.008	0.008	0.008	0.032

Group comparison: vs IR+PBS group and IR+MnTE-2-PyP⁵⁺ vs IR+MnTnHex-2-PyP⁵⁺. The *p* values were determined by Wilcoxon rank sum test (RST) and Fisher's test (Fisher) for binomial values; *p* value < 0.05 is considered significant.

HP: Hematoxylin & Eosin (H&E; structural damage). IHC: 8-hydroxy-2'-deoxyguanosine (8-OHdG; DNA-oxidation), transforming growth factor-beta 1(TGF-β1; key factor in development of lung fibrosis), hypoxia inducible factor-1 alpha (HIF-1α; alpha subunit of the transcription factor responsible for VEGF), vascular endothelial growth factor (A) (VEGF (A); growth factor responsible for angiogenesis and endothelial leakage, regulated by HIF-1α), ED-1 (ED-1 antibody for CD 68 antigen in activated rat macrophages).

Weight/ Resp. Rate (Breathing Frequencies): *p* values for pairwise (IR+PBS vs. control/treatment groups) comparison of distributions of area under the curve as measure of the entire time-course of ten weeks post-IR.

MnP-treated groups showed less histopathological damage, comprising mostly of thickening of alveolar walls, alveolar edema, accumulation of alveolar macrophages, and rarefaction of alveolar wall structures (Figs. 4 and 5, Table 1 for *p* values), but also of a high percentage of normal lung tissue. The administration of MnTnHex-2-PyP⁵⁺ and MnTE-2-PyP⁵⁺ after IR significantly reduced damage in comparison with the IR-only group ($p=0.026$ for MnTE-2-PyP⁵⁺ and $p=0.009$ for MnTnHex-2-PyP⁵⁺ vs. IR-only, RST).

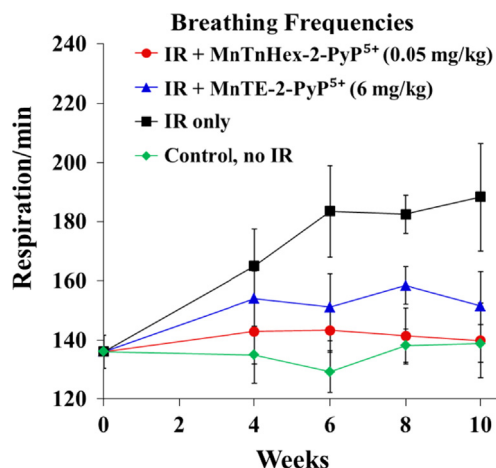


Fig. 3. The changes in breathing frequencies over 10 weeks for rats which are irradiated and treated (for 14 days starting at 2 h post-IR) with 0.05 mg/kg/day of MnTnHex-2-PyP⁵⁺ in comparison with 6 mg/kg/day of MnTE-2-PyP⁵⁺. Significantly higher breathing rates were measured in the IR only-group ($p=0.008$ vs. control group). In contrast, animals from both treatment groups (MnTnHex-2-PyP⁵⁺ 0.05 mg/kg/day and MnTE-2-PyP⁵⁺ 6 mg/kg/day) did not display any changes in breathing frequencies ($p=0.008$ for both groups vs IR only-group). Treatment with MnTnHex-2-PyP⁵⁺ after IR resulted in significantly lower breathing frequencies in comparison to the IR+MnTE-2-PyP⁵⁺ group ($p=0.032$).

Macrophage recruitment

No activation of macrophages was seen in control animals. Positive staining for ED-1 was observed in the IR-only group ($p=0.002$ vs. no IR). As seen in previous investigations [10,11], early treatment (2 h after IR) with MnTE-2-PyP⁵⁺ did not result in decreased numbers of activated macrophages ($p=0.179$ vs. IR only). On the contrary, the early post-IR treatment with MnTnHex-2-PyP⁵⁺ at a dose of 0.05 mg/kg resulted in a significantly lower activation of macrophages ($p=0.015$ vs. IR only; Table 1, Figs. 4 and 5).

DNA damage

No 8-OHdG was detected in the control group. 10 weeks post IR, a high level of DNA oxidation was seen in animals which received no MnP treatment after IR ($p=0.002$ vs. no IR). Treatment with both MnPs resulted in reduced 8-OHdG formation ($p=0.002$ for MnTE-2-PyP⁵⁺ and $p=0.009$ for MnTnHex-2-PyP⁵⁺ vs. IR only). In direct comparison between the MnTnHex-2-PyP⁵⁺ and MnTE-2-PyP⁵⁺ treatment groups, treatment with MnTE-2-PyP⁵⁺ resulted in a lower level of DNA oxidation ($p=0.015$ for MnTE-2-PyP⁵⁺ vs. MnTnHex-2-PyP⁵⁺).

TGF- β 1

No positive immunostaining for TGF- β 1 was observed in control animals. In comparison, active TGF- β 1 was significantly elevated in the IR-only group ($p=0.002$ vs. control group). The irradiated animals which were treated with either MnP post-IR exhibited the equal reduction in immunostaining for active TGF- β 1 in comparison with animals which received only PBS after irradiation (for both MnPs $p=0.002$ vs. IR only).

HIF-1 α

No positive staining for the transcription factor HIF-1 α was seen in the control group. After 10 weeks, the IR only-group displayed highly elevated levels of HIF-1 α ($p=0.002$ vs control group). Treatment with MnTE-2-PyP⁵⁺ (6 mg/kg) resulted in a significantly decreased activation of HIF-1 α ($p=0.002$ vs IR only). In contrast, with MnTnHex-2-PyP⁵⁺, starting 2 h after IR, no

significant evidence (but trend towards significance) for inhibition of HIF-1 α activation was found ($p=0.132$ vs IR only). This finding may have been confounded by a conspicuously high standard deviation in this group weakening the statistical power of analysis. Nevertheless, we were not able to determine a clear difference between MnTnHex-2-PyP⁵⁺ and MnTE-2-PyP⁵⁺ treatment in respect to activation of HIF-1 α ($p=0.24$ for MnTE-2-PyP⁵⁺ vs MnTnHex-2-PyP⁵⁺).

VEGF (A)

Vascular endothelial growth factor A, VEGF(A), is a dimeric glycoprotein. It is considered a dominant inducer of the blood vessels growth and is essential for adults during organ remodeling and diseases that involve blood vessels, such as wound healing, tumor angiogenesis, diabetic retinopathy, and age-related muscular degeneration [35]. No positive staining for VEGF (A) was seen in the control group. Significant positive staining for VEGF (A) was detected in the IR-only group ($p=0.002$ vs. control group). Animals which received MnTE-2-PyP⁵⁺ (6 mg/kg) after IR showed significantly decreased upregulation of VEGF (A) in comparison with animals which received only PBS after IR ($p=0.002$ for MnTE-2-PyP⁵⁺ vs IR only-group). Also, treatment with MnTnHex-2-PyP⁵⁺ (0.05 mg/kg) after IR resulted in decreased VEGF (A) ($p=0.009$ for MnTnHex-2-PyP⁵⁺ vs IR only-group). No difference in VEGF (A) levels was observed between the two treatment groups ($p=0.818$ for MnTE-2-PyP⁵⁺ vs MnTnHex-2-PyP⁵⁺). The strong effect of MnTnHex-2-PyP⁵⁺ on HIF-1 α -regulated VEGF by itself supports the arguments related to the high standard deviation of HIF-1 α immunohistochemistry, which might have weakened the HIF immunohistochemistry results (see above).

Discussion

Therapeutic effects of MnTnHex-2-PyP⁵⁺

To eliminate the contribution of the toxicity we undertook the study dosing a rat at 0.05 mg/kg/day for 14 days, starting at 2 h post-radiation. The therapeutic outcome at 10 weeks post-radiation and 8 weeks post-administration of MnP was impressive. At such a low dose, the MnTnHex-2-PyP⁵⁺ favorably affected the growth of rats relative to irradiated rats and to non-irradiated control rats in a similar or better way than 6 mg/kg of MnTE-2-PyP⁵⁺ (Fig. 2). The significantly higher body weight in the group which received MnTnHex-2-PyP⁵⁺ was observed in comparison with irradiated but non-treated animals (Fig. 2).

The reduction of lung injury was clearly demonstrated as MnP-based suppression of breathing frequencies (Fig. 3). Further, the lung histology (Fig. 4) indicated that fibrous masses start to form after irradiation; their growth was suppressed by both MnPs, as was the severe distortion of lung structure. Also the accumulation of alveolar macrophages, and interstitial/alveolar edema were largely reduced (Fig. 4). Both MnPs significantly suppressed oxidative stress yet at 120-fold different doses. The near full inhibition of oxidative DNA damage, i.e. formation of 8-OHdG, was demonstrated (Figs. 4 and 5). Suppression of macrophage infiltration contributed further to the suppression of oxidative stress (Figs. 4 and 5). Importantly, statistical significance has been reached in blocking the activation of alveolar macrophages after IR by 50 μ g/kg/day MnTnHex-2-PyP⁵⁺, but not by 6 mg/kg/day MnTE-2-PyP⁵⁺. Macrophages are large source of superoxide and nitric oxide which gives rise to a whole array of reactive species leading to increased secondary oxidative stress and increased activation of cellular transcription [36]. The immunohistochemical data clearly demonstrate that a cationic MnP is able to significantly affect cellular transcription and prevent detrimental fibrotic

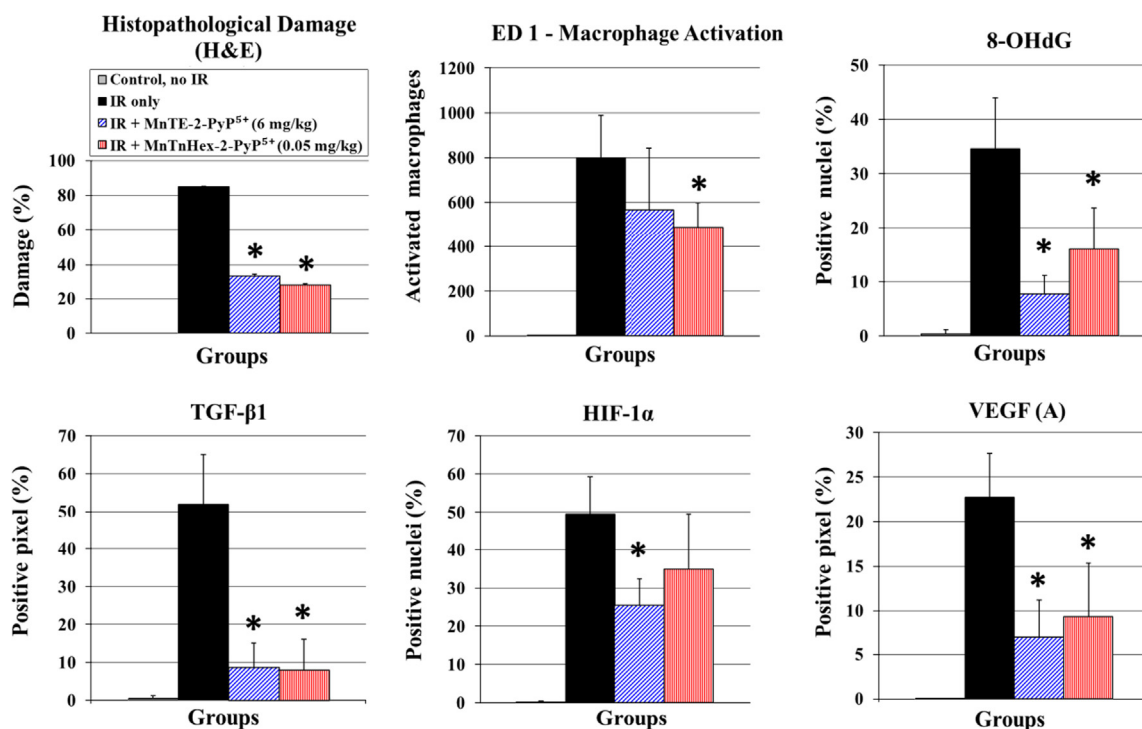


Fig. 4. The histopathology and immunohistochemistry assessed at 10 weeks post-irradiation for rats which are irradiated and treated for 14 days starting 2 h post-IR with 0.05 mg/kg/day MnTnHex-2-PyP⁵⁺ in comparison with 6 mg/kg/day MnTE-2-PyP⁵⁺. The analyses were done at 10 weeks post-IR. The effects of MnTE-2-PyP⁵⁺ and MnTnHex-2-PyP⁵⁺ on the level of histopathological damage (H&E), oxidative stress [described here by macrophage activation (ED-1) and DNA oxidative modification (8-OHdG)] and cellular transcription activity (transforming growth factor-β1 (TGF-β1), hypoxia inducible factor-1α (HIF-1α), and vascular endothelial growth factor (A) (VEGF(A)) are shown. Results are displayed as vertical bar plots with standard deviation. Stars indicate statistically significant differences between IR-only group and IR+MnP treatment groups ($p < 0.05$).

processes leading to the loss of lung function by down regulation of TGF-β1 and HIF-controlled VEGF (Figs. 4 and 5). The impact on TGF-β1 would in turn suppress oxidative stress also, as it is involved in inflammatory cell recruitment (see [Mechanistic Considerations](#)) [58]. It is important to note that MnP was administered for only 2 weeks while the therapeutic effects were still profound at 8 weeks post-drug delivery; such data provide the evidence for (i) the drug accumulation in the tissue and within cell and cellular fragments and subsequent slow release in agreement with reported pharmacokinetic studies [37]; and (ii) the catalytic nature of MnP actions.

Therapeutic effects of MnTnHex-2-PyP⁵⁺ vs its toxicity

The earlier data demonstrated a toxicity of MnTnHex-2-PyP⁵⁺ at all doses ≥ 0.6 mg/kg/day [10,11]. The lung protection was reported at 0.3 mg/kg/day but was lower relative to the effect produced by 6 mg/kg/day MnTE-2-PyP⁵⁺ [10,11]. The loss of body weight was observed with 0.3 mg/kg of MnTnHex-2-PyP⁵⁺ [10]. Other dose-dependent studies of MnTnHex-2-PyP⁵⁺ [1,2,10,38] suggest that the pro-oxidative pathways likely reduce the therapeutic efficacy of MnP when given at 0.3 mg/kg/day (Fig. 6) [10,11]. At certain threshold, the cellular levels of MnP may become too high. Under such circumstances, the higher levels of H₂O₂ will be produced by MnP (either in reaction with oxygen or superoxide, see Fig. 6 Scheme B) [39,40]. If the ability of cell to eliminate peroxide is inferior (the H₂O₂-removing enzymes down-regulated or inactivated which is often seen with cancer or gravely sick cells, see refs [38,41], H₂O₂ would be employed by MnP for the catalysis of oxidation of redox-sensitive NF-κB cysteines [giving rise to protein (R) disulfides, R-S-S-R] or glutathionylation [giving rise to glutathionylated proteins, R-S-S-G] of redox-sensitive subunits of NF-κB with consequent inhibition of its transcription. Also

MnP can catalyze the glutathionylation and subsequent inhibition of complexes I and III of mitochondrial respiration - electron transport chain, etc, with subsequent reduction in ATP production and apoptosis (Fig. 6B and summarized in [2,39,42–45]). See also discussion further below. The same pro-oxidative action is likely involved in the transient suppression of pro-inflammatory transcription factor NF-κB also, which results in limited reduction of cycling oxidative stress/inflammation and thus in beneficial therapeutic antioxidative effects [2,9,39]. MnTnHex-2-PyP⁵⁺ carries a fair micellar/surfactant character as it bears hydrophobic alkyl chains and hydrophilic positively charged pyridyl nitrogens. It therefore has the ability to damage lipid bilayers [46]. Recent data indicate, though, that ZnTnHex-2-PyP⁴⁺, the redox-inactive analog, exhibits no toxicity in darkness, while its micellar character is nearly identical to that of MnTnHex-2-PyP⁵⁺ [44,47,48]. Further studies on the mechanism of MnPs are in progress. Given the complexity of cellular pathways and MnP redox activities (due to the four biologically easily accessible oxidation states of Mn, +2, +3, +4, and +5), we are still far away from fully understanding the actions of MnPs in vivo (see refs [2,9,39] for further discussions).

Mechanistic considerations

The remarkable therapeutic efficacy of redox-active pentacationic MnPs was attributed to their impact on signaling redox-active pathways [1,2]. This was herein demonstrated by the suppression of HIF-1α transcription and downregulation of VEGF (A) and TGF-β1 (Figs. 2–4). The cross talk between NF-κB, HIF-1α, AP-1, TGF-β, NOX4 and Smad signaling pathways has been substantiated in literature [61–66]. TGF-β has a central role in fibrosis (produced by inflammatory cells and involved in their recruitment [67]). Its signal (through cell surface serine/threonine kinases)

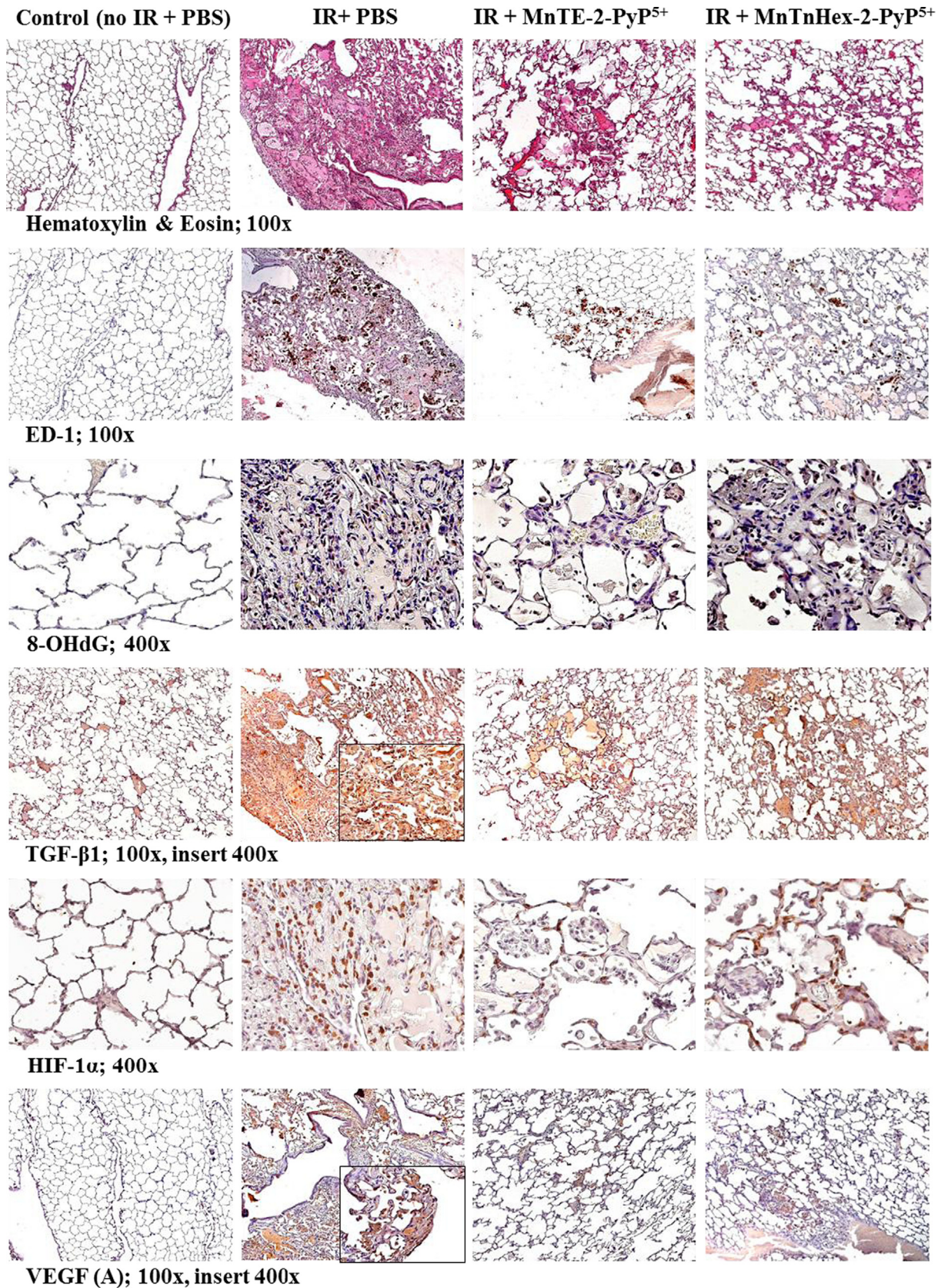


Fig. 5. The representative images of the effect of 0.05 mg/kg/day of MnTnHex-2-PyP⁵⁺ on the histopathology (H&E staining) and immunohistochemistry (ED-1, 8-OHdG, TGF-β1, HIF-1α, VEGF (A)) in comparison with 6 mg/kg/day of MnTE-2-PyP⁵⁺; treatment lasted 14 days starting at 2 h post-IR. The images were taken at 10 weeks post-IR. Magnification 100 × for H&E, TGF-β1, VEGF(A), ED-1, Magnification 400 × for 8-OHdG and HIF-1α. Groups: Control (no IR+PBS), IR+PBS (TGF-β1 and VEGF(A) images with 400 × insert), IR+MnTE-2-PyP⁵⁺ (6 mg/kg/day) [11], IR+MnTnHex-2-PyP⁵⁺ (0.05 mg/kg/day). Negative control shows normal lung structure, no positive (brown) immunostaining. IR+PBS shows large area of alveolar edema and cell infiltrates with beginning formation of fibrous masses and prominent immunostaining as well as activated macrophages (brown, localized interstitial and intra-alveolar). IR+MnTE-2-PyP⁵⁺/MnTnHex-2-PyP⁵⁺ depict focal localized damage with thickening of alveolar wall, interstitial edema, diminished immunostaining and a smaller number of localized activated macrophages.

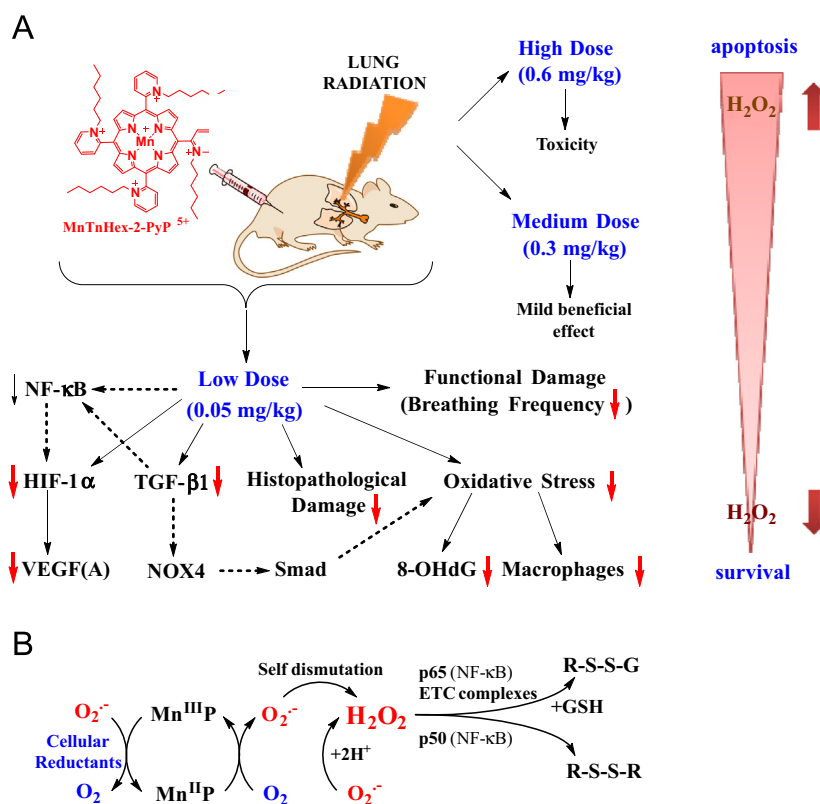


Fig. 6. Radioprotective, therapeutic effects of MnTnHex-2-PyP⁵⁺ vs its toxicity is dose-dependent. (A) The effects reported in this work. The substantial amount of literature data strongly suggest that there is a cross-talk between HIF-1 α , VEGF(A) TGF- β and NF- κ B and likely involve the effects on NADPH oxidase isoform NOX4 [16] and Smads proteins [49–52]. Effects of MnP on HIF-1 α , VEGF and NOX-4 have been reported [16,53–55]. Based on our most recent advancement in cell biology and aqueous chemistry data we believe that the in vivo mechanism of MnP is related to its redox cycling with cellular reductants and/or reactive species and oxygen as shown in Scheme B which gives rise to H₂O₂. The peroxide is in turn used by MnP to oxidize [55,56] or glutathionylate [43,45] the redox-sensitive cysteines of p50 and p65 subunits of NF- κ B. Such modifications imparted by MnP suppress the transcription of NF- κ B, perpetuating thus the inflammation. The glutathionylation of redox sensitive complexes I and III of mitochondrial electron transport chain and therefore (i) increase in O₂⁻ and its progeny production and (ii) decrease in cellular energy production may impact the HIF-1 α , VEGF(A) and TGF- β pathways and in turn the lung damage [43]. If the intracellular levels of MnP and/or peroxide are high, the magnitude of NF- κ B oxidation may be excessive and apoptosis may predominate. Such scenario likely occurred at ≥ 0.3 mg/kg/day of MnTnHex-2-PyP⁵⁺ [1,2,39,40,42,56–60]. In addition to the impact of MnP on pathways addressed in this work (red arrows), the Scheme also shows the pathways demonstrated previously to be involved in the actions of MnPs. It also includes those pathways which have not yet been explored in pulmonary radioprotection but are likely involved such as (Smads proteins).

is transduced into nucleus *via* Smads proteins [65]. Based on the cross talk between NF- κ B, HIF-1 α and TGF- β pathways and on the abundance of evidence on the effect of analogous Mn(III) *meso*-tetrakis *N*-substituted pyridylporphyrins on NF- κ B and AP-1 activation in different oxidative stress-based diseases [43,55,57,68–72], it is likely that the NF- κ B regulation of HIF-1 α transcription is at least in part controlled by the MnP-driven oxidative modification of redox-sensitive cysteines of p50 and p65 subunits of NF- κ B pathways. The action is presumably catalytic and, in addition to a MnP catalyst, involves H₂O₂ and glutathione (Scheme B of Fig. 6) [1,2,9,39,40,45]. These effects originate from the thiol oxidase- of glutathione peroxidase-like mechanisms of cationic MnPs and are presently under detailed exploration [43,45,57,69]. Such actions led to the suppression of cycling inflammation and thus suppression of secondary oxidative stress. The effects are similar to those achieved by ethyl analog, MnTE-2-PyP⁵⁺ at a 120-fold higher dose [11] (shown for comparison for both MnPs in Figs. 2–4). This remarkable enhancement in the efficacy of hexyl relative to ethyl analog has originally been attributed to the higher lipophilicity of hexyl porphyrin [18] which allows it to more easily cross plasma membrane and two mitochondrial membranes and get into the mitochondrial matrix at ~ 2.4 -fold higher level [2,7,38]. In mitochondria, the MnTnHex-2-PyP⁵⁺ acts as MnSOD. Its ability to mimic MnSOD has been most clearly demonstrated with mouse cardiomyocytes by St. Clair's group [73]. MnTnHex-2-PyP⁵⁺ also crosses the blood brain barrier

(getting into cortex and hippocampus) driven by anionic phosphates groups, and enters brain mitochondria [74]. Transport across the BBB is facilitated in much the same fashion as the transport across two mitochondrial membranes [74]. Consequently, it protects brain against radiation [75], and radiosensitizes glioblastoma multiforme D-245 MG (mouse flank sc xenograft study) to radiation and temozolomide treatment [2,76].

The impact of nearly 100 mV higher metal-centered reduction potential of MnTnHex-2-PyP⁵⁺ ($E_{1/2} = +228$ mV vs NHE for MnTE-2-PyP⁵⁺ and is +314 mV vs NHE for MnTnHex-2-PyP⁵⁺) may not be fully excluded in its differential action [2], and requires further investigations. Based on our present knowledge, we believe that the beneficial therapeutic effects of this and other cationic Mn(III) *N*-substituted pyridylporphyrins originate likely from the interplay of their lipophilicities and redox-activities. For example, once it is distributed within cell, the higher the $E_{1/2}$, the easier MnP is reduced with cellular reductant; consequently it prefers to stay in +2 oxidation state. This suppresses or precludes its ability to redox cycle back to Mn +3 or +4 oxidation states in order to exert catalytic action in regulation of redox-sensitive NF- κ B/HIF pathways [2,34,42,77]. The action/s of MnTnHex-2-PyP⁵⁺, which contribute to the pulmonary radioprotection, are summarized in Fig. 6. In addition to NF- κ B, MnP is also able to inhibit AP-1 as reported in skin carcinogenesis model [72] and HIF-1 α transcription factor as reported here and in 4T1 breast cancer model [78]. The PI3K/AKT pathway is reportedly involved in AP-1 suppression by MnP [72], and is linked to NF- κ B, HIF pathways

and mTOR pathways. The former is known to be involved in the activation of mTOR which in turn regulates cell growth, cell proliferation, cell motility, cell survival, protein synthesis, and transcription. Thus far, the most widely explored the *in vivo* impact of MnP on redox-sensitive proteins relates to the studies of the oxidation of cysteines of NF- κ B and complexes I, III, and IV of mitochondrial electron transport chain in lymphoma cellular model [43,79]. The critical importance of such studies is reflected in the fact that thiol modifications are regarded as major signaling events [41,80]. The impact of MnP on NF- κ B in CNS injuries [71,81], and diabetes has been addressed also [12,55,56,58,82].

The additional benefit of a lipophilic MnTnHex-2-PyP⁵⁺, relative to a hydrophilic and equally redox-active analog MnTE-2-PyP⁵⁺, lies in the fact that 120-fold less drug needs to be synthesized in the case of former. That could in turn greatly reduce costs of GMP-based drug synthesis. Even more importantly, it is easier to formulate 4 mg of MnTnHex-2-PyP⁵⁺ relative to the formulation of ~500 mg of MnTE-2-PyP⁵⁺ for a daily administration to an adult whose weight averages ~80 kg. Of note, MnTE-2-PyP⁵⁺ was GMP-synthesized and Drug Master File filed. A good safety/toxicity profile was demonstrated [83].

Conclusion

Our data demonstrate a remarkable rat lung radioprotection exerted by a lipophilic MnTnHex-2-PyP⁵⁺. Under same experimental conditions a similar magnitude of protection was observed with MnTnHex-2-PyP⁵⁺ at 50 μ g/kg/day (given for 14 days, starting at 2 h post-radiation) as with 120-fold higher dose of hydrophilic MnTE-2-PyP⁵⁺. Both Mn porphyrins prevent direct oxidative damage of biomolecules as demonstrated with large suppression of 8-OHdG formation. Further, they impact the HIF-1 α /VEG (A)/TGF- β 1 redox-sensitive signaling pathways, presumably involving NF- κ B, whereby reducing secondary oxidative stress and in turn preventing irradiation-based lung fibrosis and loss of its function. Finally, the MnP-driven reduction in recruitment of macrophages – major source of reactive species – contributed largely to the suppression of oxidative stress.

Once the drug reaches clinics, there is a significant advantage in formulating a low amount of it. The formulation of 4 mg of a drug needed for daily administration of MnTnHex-2-PyP⁵⁺ to an 80 kg-adult should not present a problem, while the formulation of ~500 mg of a hydrophilic MnTE-2-PyP⁵⁺ could be challenging.

Acknowledgments

Authors (ZV, IBH, AT, JSR, BGF, KF) are grateful for financial support to NIH for Grant no. NIH-U19-AI-067798. IBH and AT also acknowledge IBH General Research Funds.

References

- [1] I. Batinic-Haberle, J.S. Reboucas, I. Spasojevic, Superoxide dismutase mimics: chemistry, pharmacology, and therapeutic potential, *Antioxid Redox Signal* 13 (6) (2010) 877–918.
- [2] I. Batinic-Haberle, A. Tovmasyan, E.R. Roberts, Z. Vujaskovic, K.W. Leong, I. Spasojevic, SOD Therapeutics: latest insights into their structure-activity relationships and impact on the cellular redox-based signaling pathways, *Antioxid Redox Signal* (2013), <http://dx.doi.org/10.1089/ars.2012.5147>.
- [3] R.M. Davis, J.B. Mitchell, M.C. Krishna, Nitroxides as cancer imaging agents, *Anti-Cancer Agents Med. Chem.* 11 (4) (2011) 347–358.
- [4] J.F. Arambula, C. Preihs, D. Borthwick, D. Magda, J.L. Sessler, Texaphyrins: tumor localizing redox active expanded porphyrins, *Anticancer Agents Med. Chem.* 11 (2) (2011) 222–232.
- [5] R.A. Floyd, H.K. Chandru, T. He, R. Towner, Anti-cancer activity of nitrones and observations on mechanism of action, *Anticancer Agents Med. Chem.* 11 (4) (2011) 373–379.

- [6] R.A. Rosenthal, B. Fish, R.P. Hill, K.D. Huffman, Z. Lazarova, J. Mahmood, M. Medhora, R. Molthen, J.E. Moulder, S.T. Sonis, et al., Salen Mn complexes mitigate radiation injury in normal tissues, *Anticancer Agents Med Chem* 11 (4) (2011) 359–372.
- [7] I. Batinic-Haberle, Z. Rajic, A. Tovmasyan, J.S. Reboucas, X. Ye, K.W. Leong, M.W. Dewhirst, Z. Vujaskovic, L. Benov, I. Spasojevic, Diverse functions of cationic Mn(III) N-substituted pyridylporphyrins, recognized as SOD mimics, *Free Radic. Biol. Med.* 51 (5) (2011) 1035–1053.
- [8] A. Tovmasyan, H. Sheng, T. Weitner, A. Arulpragasam, M. Lu, D.S. Warner, Z. Vujaskovic, I. Spasojevic, I. Batinic-Haberle, Design, mechanism of action, bioavailability and therapeutic effects of Mn porphyrin-based redox modulators, *Med. Principles Pract.* 22 (2) (2013) 103–130.
- [9] I. Batinic Haberle, A. Tovmasyan, I. Spasojevic, The complex mechanistic aspects of redox-active compounds, commonly regarded as SOD mimics, *Biolnorg. React. Mech.* (2013), <http://dx.doi.org/10.1515/irm-2013-0004>.
- [10] B. Gauter-Fleckenstein, K. Fleckenstein, K. Owzar, C. Jiang, I. Batinic-Haberle, Z. Vujaskovic, Comparison of two Mn porphyrin-based mimics of superoxide dismutase in pulmonary radioprotection, *Free Radic. Biol. Med.* 44 (6) (2008) 982–989.
- [11] B. Gauter-Fleckenstein, K. Fleckenstein, K. Owzar, C. Jiang, J.S. Reboucas, I. Batinic-Haberle, Z. Vujaskovic, Early and late administration of MnTE-2-PyP⁵⁺ in mitigation and treatment of radiation-induced lung damage, *Free Radic. Biol. Med.* 48 (8) (2010) 1034–1043.
- [12] I. Batinic-Haberle, I. Spasojevic, H.M. Tse, A. Tovmasyan, Z. Rajic, D.K. Clair, Z. Vujaskovic, M.W. Dewhirst, J.D. Piganelli, Design of Mn porphyrins for treating oxidative stress injuries and their redox-based regulation of cellular transcriptional activities, *Amino Acids* 42 (1) (2012) 95–113.
- [13] I.L. Jackson, L. Chen, I. Batinic-Haberle, Z. Vujaskovic, Superoxide dismutase mimetic reduces hypoxia-induced O₂^{•-}, TGF- β , and VEGF production by macrophages, *Free Radic. Res.* 41 (1) (2007) 8–14.
- [14] Z.N. Rabbani, I. Batinic-Haberle, M.S. Anscher, J. Huang, B.J. Day, E. Alexander, M.W. Dewhirst, Z. Vujaskovic, Long-term administration of a small molecular weight catalytic metalloporphyrin antioxidant, AEOL 10150, protects lungs from radiation-induced injury, *Int. J. Radiat. Oncol. Biol. Phys.* 67 (2) (2007) 573–580.
- [15] Z.N. Rabbani, F.K. Salahuddin, P. Yarmolenko, I. Batinic-Haberle, B.A. Thrasher, B. Gauter-Fleckenstein, M.W. Dewhirst, M.S. Anscher, Z. Vujaskovic, Low molecular weight catalytic metalloporphyrin antioxidant AEOL 10150 protects lungs from fractionated radiation, *Free Radic. Res.* 41 (11) (2007) 1273–1282.
- [16] Z.N. Rabbani, I. Spasojevic, X. Zhang, B.J. Moeller, S. Haberle, J. Vasquez-Vivar, M.W. Dewhirst, Z. Vujaskovic, I. Batinic-Haberle, Antiangiogenic action of redox-modulating Mn(III) meso-tetrakis(N-ethylpyridinium-2-yl)porphyrin, MnTE-2-PyP(5⁺), via suppression of oxidative stress in a mouse model of breast tumor, *Free Radic. Biol. Med.* 47 (7) (2009) 992–1004.
- [17] M.C. Garofalo, A.A. Ward, A.M. Farese, A. Bennett, C. Taylor-Howell, W. Cui, A. Gibbs, K.L. Prado, T.J.A. Macvittie, Pilot study in rhesus macaques to assess the treatment efficacy of a small molecular weight catalytic metalloporphyrin antioxidant (AEOL 10150) in mitigating radiation-induced lung damage, *Health Phys.* 106 (1) (2014) 73–83.
- [18] I. Kos, J.S. Reboucas, G. DeFreitas-Silva, D. Salvemini, Z. Vujaskovic, M.W. Dewhirst, I. Spasojevic, I. Batinic-Haberle, Lipophilicity of potent porphyrin-based antioxidants: comparison of ortho and meta isomers of Mn(III) N-alkylpyridylporphyrins, *Free Radic. Biol. Med.* 47 (1) (2009) 72–78.
- [19] J.M. Pollard, J.S. Reboucas, A. Durazo, I. Kos, F. Fike, M. Panni, E.B. Gralla, J.S. Valentine, I. Batinic-Haberle, R.A. Gatti, Radioprotective effects of manganese-containing superoxide dismutase mimics on ataxia-telangiectasia cells, *Free Radic. Biol. Med.* 47 (3) (2009) 250–260.
- [20] I. Batinic-Haberle, J.S. Reboucas, L. Benov, I. Spasojevic, Chemistry, biology and medical effects of water soluble metalloporphyrins, in: K.M. Kadish, K.M. Smith, R. Guillard (Eds.), *Handbook of Porphyrin Science*, vol. 11, World Scientific, Singapore, 2011, pp. 291–393.
- [21] I. Spasojevic, I. Batinic-Haberle, Superoxide dismutase mimics, in: K. Pantopoulos, H. Schipper (Eds.), *Principles of Free Radical Biomedicine*, vol. II, Nova Science, Publisher, Inc., New York, USA, 2012, pp. 101–128.
- [22] L. Benov, J. Craik, I. Batinic-Haberle, Protein damage by photo-activated Zn(II) N-alkylpyridylporphyrins, *Amino Acids* (2010).
- [23] A. Drobyshevsky, K. Luo, M. Derrick, L. Yu, H. Du, P.V. Prasad, J. Vasquez-Vivar, I. Batinic-Haberle, S. Tan, Motor deficits are triggered by reperfusion-reoxygenation injury as diagnosed by MRI and by a mechanism involving oxidants, *J. Neurosci.* 32 (16) (2012) 5500–5509.
- [24] H. Saba, I. Batinic-Haberle, S. Munusamy, T. Mitchell, C. Licht, J. Megyesi, L.A. MacMillan-Crow, Manganese porphyrin reduces renal injury and mitochondrial damage during ischemia/reperfusion, *Free Radic. Biol. Med.* 42 (10) (2007) 1571–1578.
- [25] Cline J.M., Dugan G., Bourland D., Perry D.L., Stitzel J.D., Weaver A.A., Jiang C., Owzar K., Spasojevic I., Batinic-Haberle I. et al., Post-irradiation treatment with MnTnHex-2-PyP⁵⁺ mitigates radiation pneumonitis and fibrosis in the lungs of non-human primates after whole-thorax exposure to ionizing radiation, *Radiat. Res.* (2014) in Revision.
- [26] I. Batinic-Haberle, I. Spasojevic, R.D. Stevens, P. Hambright, I. Fridovich, Manganese(III) meso-tetrakis(ortho-N-alkylpyridyl)porphyrins. Synthesis, characterization, and catalysis of O-2 (center dot-) dismutation, *J. Chem. Soc. Dalton Trans.* 13 (2002) 2689–2696.
- [27] K. Fleckenstein, L. Zgonjanin, L. Chen, Z. Rabbani, I.L. Jackson, B. Thrasher, J. Kirkpatrick, W.M. Foster, Z. Vujaskovic, Temporal onset of hypoxia and

- oxidative stress after pulmonary irradiation, *Int. J. Radiat. Oncol. Biol. Phys.* 68 (1) (2007) 196–204.
- [28] T. Ashcroft, J.M. Simpson, V. Timbrell, Simple method of estimating severity of pulmonary fibrosis on a numerical scale, *J. Clin. Pathol.* 41 (4) (1988) 467–470.
- [29] S.M. Hsu, L. Raine, H. Fanger, Use of avidin–biotin–peroxidase complex (ABC) in immunoperoxidase techniques: a comparison between ABC and unlabeled antibody (PAP) procedures, *J. Histochem. Cytochem.* 29 (4) (1981) 577–580.
- [30] A. Agresti, *Categorical data analysis*, Wiley, New York (1990) 59–66.
- [31] J. Hajek, Z. Sidak, K. Pranab, *Theory of Rank Tests*, Academic Press, San Diego, 1999.
- [32] R Foundation for Statistical Computing, Vienna, Austria, 2007.
- [33] A.G. Tovmasyan, Z. Rajic, I. Spasojevic, J.S. Reboucas, X. Chen, D. Salvemini, H. Sheng, D.S. Warner, L. Benov, I. Batinic-Haberle, Methoxy-derivatization of alkyl chains increases the in vivo efficacy of cationic Mn porphyrins. Synthesis, characterization, SOD-like activity, and SOD-deficient *E. coli* study of meta Mn (III) N-methoxyalkylpyridylporphyrins, *Dalton Trans.* 40 (16) (2011) 4111–4121.
- [34] X. Ye, D. Fels, A. Tovmasyan, K.M. Aird, C. Dedeugd, J.L. Allensworth, I. Kos, W. Park, I. Spasojevic, G.R. Devi, et al., Cytotoxic effects of Mn(III) N-alkylpyridylporphyrins in the presence of cellular reductant, ascorbate, *Free Radic. Res.* 45 (11–12) (2011) 1289–1306.
- [35] L. Zeng, Q. Xiao, M. Chen, A. Margariti, D. Martin, A. Ivetic, H. Xu, J. Mason, W. Wang, G. Cockerill, et al., Vascular endothelial cell growth-activated XBP1 splicing in endothelial cells is crucial for angiogenesis, *Circulation* 127 (16) (2013) 1712–1722.
- [36] H.J. Forman, M. Torres, Redox signaling in macrophages, *Mol. Asp. Med.* 22 (4–5) (2001) 189–216.
- [37] T. Weitner, I. Kos, H. Sheng, A. Tovmasyan, J.S. Reboucas, P. Fan, D.S. Warner, Z. Vujaskovic, I. Batinic-Haberle, I. Spasojevic, Comprehensive pharmacokinetic studies and oral bioavailability of two Mn porphyrin-based SOD mimics, MnTE-2-PyP(5⁺) and MnTnHex-2-PyP(5⁺), *Free Radic. Biol. Med.* 58 (2013) 73–80.
- [38] S. Miriyala, I. Spasojevic, A. Tovmasyan, D. Salvemini, Z. Vujaskovic, D. Clair, I. Batinic-Haberle, Manganese superoxide dismutase, MnSOD and its mimics, *Biochim. Biophys. Acta* 1822 (5) (2012) 794–814.
- [39] D.K. Ali, M. Oriowo, A. Tovmasyan, I. Batinic-Haberle, L. Benov, Late administration of Mn porphyrin-based SOD mimic enhances diabetic complications, *Redox Biol.* 1 (1) (2013) 457–466.
- [40] J.O. Archambeau, A. Tovmasyan, R.D. Pearlsten, J.D. Crapo, I. Batinic-Haberle, Superoxide dismutase mimic, MnTE-2-PyP5⁺ ameliorates acute and chronic proctitis following focal proton irradiation of the rat Rectum, *Redox Biol.* 1 (1) (2013) 599–607.
- [41] Y. Wang, J. Yang, J. Yi, Redox sensing by proteins: oxidative modifications on cysteines and the consequent events, *Antioxid Redox Signal* 16 (7) (2012) 649–657.
- [42] M.K. Evans, A. Tovmasyan, I. Batinic-Haberle, G.R. Devi, Mn Porphyrin in combination with ascorbate acts as a pro-oxidant and mediates caspase-independent cancer cell death, *Free Radic. Biol. Med.* 68 (2014) 302–314.
- [43] M.C. Jaramillo, M.M. Briehl, I. Batinic-Haberle, M.E. Tome, Inhibition of the electron transport chain via the pro-oxidative activity of manganese porphyrin-based SOD mimetics modulates bioenergetics and enhances the response to chemotherapy, *Free Radic. Biol. Med.* 65 (2013) S25.
- [44] A. Tovmasyan, J.S. Reboucas, L. Benov, Simple biological systems for assessing the activity of superoxide dismutase mimics, *Antioxid Redox Signal* (2013), <http://dx.doi.org/10.1089/ars.2013.5576>.
- [45] A. Tovmasyan, T. Weitner, M. Jaramillo, R. Wedmann, E. Roberts, K.W. Leong, M. Filipovic, I. Ivanovic-Burmazovic, L. Benov, M. Tome, et al., We have come a long way with Mn porphyrins: from superoxide dismutation to H₂O₂-driven pathways, *Free Rad. Biol. Med.* 65 (2013) S133.
- [46] A. Okado-Matsumoto, I. Batinic-Haberle, I. Fridovich, Complementation of SOD-deficient *Escherichia coli* by manganese porphyrin mimics of superoxide dismutase activity, *Free Radic. Biol. Med.* 37 (3) (2004) 401–410.
- [47] L. Benov, J. Craik, I. Batinic-Haberle, The potential of Zn(II) N-alkylpyridylporphyrins for anticancer therapy, *Anticancer Agents Med. Chem.* 11 (2) (2011) 233–241.
- [48] R. Ezzeddine, A. Al-Banaw, A. Tovmasyan, J.D. Craik, I. Batinic-Haberle, L.T. Benov, Effect of molecular characteristics on cellular uptake, subcellular localization and phototoxicity of Zn(II) N-alkylpyridylporphyrins, *J. Biol. Chem.* (2013), <http://dx.doi.org/10.1074/jbc.M113.511642>.
- [49] L. Wu, X. Huang, L. Li, H. Huang, R. Xu, W. Luyten, Insights on biology and pathology of HIF-1alpha/-2alpha, TGFbeta/BMP, Wnt/beta-catenin, and NF-kappaB pathways in osteoarthritis, *Curr. Pharm. Des.* 18 (22) (2012) 3293–3312.
- [50] S.R. Shiou, Y. Yu, Y. Guo, M. Westerhoff, L. Lu, E.O. Petrof, J. Sun, E.C. Claud, Oral administration of TGF-beta1 protects the immature gut from injury via Smad-dependent suppression of epithelial NF-kappaB signaling and pro-inflammatory cytokine production, *J. Biol. Chem.* 288 (48) (2013) 34757–34766.
- [51] A. Kauppinen, T. Suuronen, J. Ojala, K. Kaarniranta, A. Salminen, Antagonistic crosstalk between NF-kappaB and SIRT1 in the regulation of inflammation and metabolic disorders, *Cell Signal* 25 (10) (2013) 1939–1948.
- [52] I.L. Jackson, I. Batinic-Haberle, P. Sonveaux, M.W. Dewhirst, Z. Vujaskovic, ROS production and angiogenic regulation by macrophages in response to heat therapy, *Int. J. Hyperthermia* 22 (4) (2006) 263–273.
- [53] S.K. Pazhanisamy, H. Li, Y. Wang, I. Batinic-Haberle, D. Zhou, NADPH oxidase inhibition attenuates total body irradiation-induced haematopoietic genomic instability, *Mutagenesis* 26 (3) (2011) 431–435.
- [54] E.J. Moon, P. Sonveaux, P.E. Porporato, P. Danhier, B. Gallez, I. Batinic-Haberle, Y.C. Nien, T. Schroeder, M.W. Dewhirst, NADPH oxidase-mediated reactive oxygen species production activates hypoxia-inducible factor-1 (HIF-1) via the ERK pathway after hyperthermia treatment, *Proc. Natl. Acad. Sci. USA* 107 (47) (2010) 20477–20482.
- [55] J.D. Piganelli, S.C. Flores, C. Cruz, J. Koepf, I. Batinic-Haberle, J. Crapo, B. Day, R. Kachadourian, R. Young, B. Bradley, et al., A metalloporphyrin-based superoxide dismutase mimic inhibits adoptive transfer of autoimmune diabetes by a diabetogenic T-cell clone, *Diabetes* 51 (2) (2002) 347–355.
- [56] M.M. Delmastro-Greenwood, H.M. Tse, J.D. Piganelli, Effects of metalloporphyrins on reducing inflammation and autoimmunity, *Antioxid Redox Signal* (2013), <http://dx.doi.org/10.1089/ars.2013.5257>.
- [57] M.C. Jaramillo, M.M. Briehl, J.D. Crapo, I. Batinic-Haberle, M.E. Tome, Manganese porphyrin, MnTE-2-PyP5⁺, acts as a pro-oxidant to potentiate glucocorticoid-induced apoptosis in lymphoma cells, *Free Radic. Biol. Med.* 52 (8) (2012) 1272–1284.
- [58] M.M. Delmastro-Greenwood, T. Votyakova, E. Goetzman, M.L. Marre, D.M. Previte, A. Tovmasyan, I. Batinic-Haberle, M. Trucco, J.D. Piganelli, Mn porphyrin regulation of aerobic glycolysis: implications on the activation of diabetogenic immune cells, *Antioxid Redox Signal* (2013), <http://dx.doi.org/10.1089/ars.2012.5167>.
- [59] H.M. Tse, M.J. Milton, J.D. Piganelli, Mechanistic analysis of the immunomodulatory effects of a catalytic antioxidant on antigen-presenting cells: implication for their use in targeting oxidation-reduction reactions in innate immunity, *Free Radic. Biol. Med.* 36 (2) (2004) 233–247.
- [60] H.M. Tse, T.C. Thayer, C. Steele, C.M. Cuda, L. Morel, J.D. Piganelli, C.E. Mathews, NADPH oxidase deficiency regulates Th lineage commitment and modulates autoimmunity, *J. Immunol.* 185 (9) (2010) 5247–5258.
- [61] M.M. Chaturvedi, B. Sung, V.R. Yadav, R. Kannappan, B.B. Aggarwal, NF-kappaB addiction and its role in cancer: 'one size does not fit all', *Oncogene* 30 (14) (2011) 1615–1630.
- [62] J. Wilczynski, M. Duechler, M. Czyn, Targeting NF-kappaB and HIF-1 pathways for the treatment of cancer: part II, *Arch. Immunol. Ther. Exp. (Warsz)* 59 (4) (2011) 301–307.
- [63] K.M. Oliver, J.F. Garvey, C.T. Ng, D.J. Veale, U. Fearon, E.P. Cummins, C.T. Taylor, Hypoxia activates NF-kappaB-dependent gene expression through the canonical signaling pathway, *Antioxid Redox Signal* 11 (9) (2009) 2057–2064.
- [64] I. Fernandez, A. Martin-Garrido, R.E. Clempus, W. Seidel-Rogol, A. Amanso, B. Lassegue, K.K. Griendling, A.S. Martin, TGF-beta mediates focal adhesion maturation by a Smad/Nox4-dependent mechanism that involves regulation of Hsp27 and Hic5, *Free Radic. Biol. Med.* 65 (2013) S157.
- [65] K.C. Flanders, Smad3 as a mediator of the fibrotic response, *Int. J. Exp. Pathol.* 85 (2) (2004) 47–64.
- [66] M. Bitzer, G. von Gersdorff, D. Liang, A. Dominguez-Rosales, A.A. Beg, M. Rojkind, E.P. Bottinger, A mechanism of suppression of TGF-beta/SMAD signaling by NF-kappa B/RelA, *Genes Dev.* 14 (2) (2000) 187–197.
- [67] T. Yamamoto, S. Imoto, Y. Sekine, K. Sugiyama, T. Akimoto, A. Muraguchi, T. Matsuda, Involvement of NF-kappaB in TGF-beta-mediated suppression of IL-4 signaling, *Biochem. Biophys. Res. Commun.* 313 (3) (2004) 627–634.
- [68] I. Batinic-Haberle, S.T. Keir, Z. Rajic, A. Tovmasyan, D.D. Bigner, Lipophilic Mn porphyrins in the treatment of brain tumors, *Free Radic. Biol. Med.* 51 (2011) S119.
- [69] M.C. Jaramillo, J.B. Frye, J.D. Crapo, M.M. Briehl, M.E. Tome, Increased manganese superoxide dismutase expression or treatment with manganese porphyrin potentiates dexamethasone-induced apoptosis in lymphoma cells, *Cancer Res.* 69 (13) (2009) 5450–5457.
- [70] H. Sheng, R.E. Chaparro, T. Sasaki, M. Izutsu, R.D. Pearlstein, A. Tovmasyan, D.S. Warner, Metalloporphyrins as therapeutic catalytic oxidoreductants in central nervous system disorders, *Antioxid Redox Signal* (2013), <http://dx.doi.org/10.1089/ars.2013.5413>.
- [71] H. Sheng, W. Yang, S. Fukuda, H.M. Tse, W. Paschen, K. Johnson, I. Batinic-Haberle, J.D. Crapo, R.D. Pearlstein, J. Piganelli, et al., Long-term neuroprotection from a potent redox-modulating metalloporphyrin in the rat, *Free Radic. Biol. Med.* 47 (7) (2009) 917–923.
- [72] Y. Zhao, L. Chaiswing, T.D. Oberley, I. Batinic-Haberle, W. Clair, C.J. Epstein, D. Clair, A mechanism-based antioxidant approach for the reduction of skin carcinogenesis, *Cancer Res.* 65 (4) (2005) 1401–1405.
- [73] M. Panchatcharam, N. Hendrix, A. Tovmasyan, I. Batinic-Haberle, D.S. Clair, S. Miriyala, MnTnBuOE-2-PyP5⁺ improves respiratory function and inhibits RAGE induced reactive oxygen species generation, *Free Radic. Biol. Med.* 65 (2013) S129–S130.
- [74] I. Spasojevic, T. Weitner, A. Tovmasyan, H. Sheng, S. Miriyala, D. Leu, Z. Rajic, D.S. Warner, D.K. Clair, T.T. Huang, et al., Pharmacokinetics, brain hippocampus and cortex, and mitochondrial accumulation of a new generation of lipophilic redox-active therapeutic, Mn(III) Meso Tetrakis(N-n-butoxyethylpyridinium-2-yl) porphyrin, MnTnBuOE-2-PyP5⁺, in comparison with its ethyl and N-hexyl Analogs, MnTE-2-PyP5⁺ and MnTnHex-2-PyP5⁺, *Free Radic. Biol. Med.* 65 (2013) S132.
- [75] C.M. Beausejour, L. Palacio, O. Le, I. Batinic-Haberle, N.E. Sharpless, S. Marcoux, C. Laverdiere, Decreased Neurogenesis following Exposure to Ionizing Radiation: A Role for p16^{INK4a}-Induced Senescence. *Cell Senescence in Cancer and Ageing*, Wellcome Trust Genome Campus, Hinxton, Cambridge, UK, 2013.
- [76] I. Batinic-Haberle, A. Tovmasyan, T. Weitner, Z. Rajic, S.T. Keir, T.T. Huang, D. Leu, D.H. Weitzel, C.M. Beausejour, S. Miriyala, et al., Mechanistic considerations of the therapeutic Effects of Mn porphyrins, commonly regarded as SOD mimics, in anticancer therapy: lessons from brain and lymphoma studies, *Free Radic. Biol. Med.* 65 (2013) S120–S121.

- [77] I. Spasojevic, I. Kos, L.T. Benov, Z. Rajic, D. Fels, C. Dedeugd, X. Ye, Z. Vujaskovic, J.S. Reboucas, K.W. Leong, et al., Bioavailability of metalloporphyrin-based SOD mimics is greatly influenced by a single charge residing on a Mn site, *Free Radic. Res.* 45 (2) (2011) 188–200.
- [78] B.J. Moeller, Y. Cao, C.Y. Li, M.W. Dewhirst, Radiation activates HIF-1 to regulate vascular radiosensitivity in tumors: role of reoxygenation, free radicals, and stress granules, *Cancer Cell* 5 (5) (2004) 429–441.
- [79] M.R. Weaver, S. Smith, S. Venkataraman, R.E. Oberley-Deegan, MnTE-2-PyP inhibits prostate tumor growth and metastasis by inhibiting p300 activity, *Free Radic. Biol. Med.* 65 (2013) S22.
- [80] E.M. Allen, J.J. Mieyal, Protein-thiol oxidation and cell death: regulatory role of glutaredoxins, *Antioxid Redox Signal* 17 (12) (2012) 1748–1763.
- [81] H. Sheng, I. Spasojevic, H.M. Tse, J.Y. Jung, J. Hong, Z. Zhang, J.D. Piganelli, I. Batinic-Haberle, D.S. Warner, Neuroprotective efficacy from a lipophilic redox-modulating Mn(III) N-Hexylpyridylporphyrin, MnTnHex-2-PyP: rodent models of ischemic stroke and subarachnoid hemorrhage, *J. Pharmacol. Exp. Ther.* 338 (3) (2011) 906–916.
- [82] R. Bottino, A.N. Balamurugan, H. Tse, C. Thirunavukkarasu, X. Ge, J. Profozich, M. Milton, A. Ziegenfuss, M. Trucco, J.D. Piganelli, Response of human islets to isolation stress and the effect of antioxidant treatment, *Diabetes* 53 (10) (2004) 2559–2568.
- [83] S.C. Gad, D.W. Sullivan, J.D. Crapo, C.B.A. Spainhour, Nonclinical safety assessment of MnTE-2-PyP, a manganese porphyrin, *Int. J. Toxicol.* 32 (4) (2013) 274–287.